

Infrared transient grating and photon echo spectroscopy of oxygen vibrational modes in amorphous silicon thin films

Jon-Paul R. Wells,^{1,*} P. Jonathan Phillips,² Nicolae Tomozeiu,³ Frans H. P. M. Habraken,³ and Jaap I. Dijkhuis⁴

¹*Department of Physics and Astronomy, University of Sheffield, S3 7RH, United Kingdom*

²*Department of Physics, Heriot-Watt University, Edinburgh E14 4AS, United Kingdom*

³*Surfaces, Interfaces and Devices, Debye Institute, University of Utrecht, P.O. Box 80000, TA 3508 Utrecht, The Netherlands*

⁴*Atom Optics and Ultrafast Dynamics, Debye Institute, University of Utrecht, P.O. Box 80000, TA 3508 Utrecht, The Netherlands*

(Received 27 January 2003; published 29 September 2003)

We report on picosecond coherent transient spectroscopy on the asymmetric stretching mode in a -SiO_{0.1} thin films using the Dutch free-electron laser FELIX. A fast 10-K lifetime of 2.8 ps is obtained using laser-induced transient grating spectroscopy. Its thermal behavior suggests relaxation into two accepting modes possibly via the symmetric stretch mode of the Si-O-Si complex. Two-pulse photon echo measurements reveal phase dynamics with both an excitation density and temperature dependence, suggesting the presence of nonequilibrium Si-Si phonons. The temperature-dependent component of the pure dephasing may be attributable to two-phonon elastic scattering. From the probe pulse diffraction efficiency, a value of the nonlinear refractive index has been determined to be $n_2 = 3.73 \times 10^{-3} \text{ cm}^2/\text{GW}$.

DOI: 10.1103/PhysRevB.68.115207

PACS number(s): 61.43.Dq, 78.47.+p, 78.30.Ly, 63.50.+x

I. INTRODUCTION

The optical properties of Si/SiO₂ nanostructures are very promising for future opto-electronic applications. Silicon nanocrystals embedded in a SiO₂ matrix exhibit efficient photoluminescence due to quantum-confined exciton recombination in the wavelength range between 500 and 1100 nm largely because dangling bonds are passivated and nonradiative recombination is effectively suppressed.¹ On the other hand, suboxide-related centers are thought to play a crucial role in the optical properties of the Si/SiO₂ nanostructures² and are even held responsible for the observation of optical gain in silicon nanocrystals.³ In this context, silicon suboxides (SiO_x) represent an interesting class of materials because they phase separate into a mixture of Si and SiO₂.⁴ This phase separation is thought to proceed by activated diffusion of bridging oxygen atoms preferentially to the oxygen-rich regions.⁵ Recently it has been made possible to study the dynamics of defect vibrations utilizing advances in intense, tunable infrared (ir) light pulses made available from a free-electron laser (FEL) and optical parametric oscillators and generators. We have commenced a study at the Dutch FEL facility FELIX, on the Si-O-Si complex in amorphous Si diluted with oxygen, in order to demonstrate that unique microscopic information can be obtained using ultrafast coherent vibrational spectroscopy. We identify the fundamental vibrational relaxation processes of the asymmetric stretch vibration of the Si-O-Si complex. Our resonant technique is very selective, and therefore quite promising in silicon suboxides to elucidate the phase separation processes and perhaps even to selectively induce the phase separation by strong resonant ir radiation and in Si/SiO₂ nanostructures to further assess the nature of the optical centers.

There are few previous studies of the dynamics of vibrations in amorphous silicon. Our recent work has concentrated upon studies of vibrational relaxation in hydrogenated and deuterated amorphous silicon.^{6,7} These previous studies es-

tablished the significance of studying the vibrational dynamics in amorphous materials since subtle differences in the vibrational decay pathways can be shown to be responsible for dramatic differences in the macroscopic properties of the materials. In this study, we concentrate on a -Si:O_{0.1}. Oxygen in amorphous silicon^{8,9} forms a twofold bridging bond between two silicon atoms. As such, the oxygen atom resides in a site with a C_{2v} point-group symmetry. Consequently there are three modes associated with this defect corresponding to the normal modes of vibration of the interstitial impurity system. These are the asymmetric stretching mode, which is a motion at right angles to the twofold axis in a direction parallel to a line joining the two Si atoms, the symmetric stretching mode (or bending mode—along the direction of the bisector of the Si-O-Si bond angle) and a rocking mode, which is best described as an out-of-plane mode in a direction that is perpendicular to the plane of the Si-O-Si bond. In this initial study we have concentrated upon the population decay and phase relaxation of the asymmetric stretch mode of the Si-O-Si complex which has the largest dipole moment and is the most readily accessible having the highest frequency of vibration.

II. EXPERIMENT

The samples consist of a 1.0- μm -thick a -SiO_{0.1} layer grown by reactive magnetron sputtering on a double-polished 250- μm c -Si substrate. All of the data collected here were performed using samples dipped in HF to remove the native SiO₂, although samples that had not undergone this treatment showed no substantial difference in their behavior. Assessment of the samples was performed using infrared (linear) absorption with a N₂-purged Nicolet Fourier-transform infrared (FTIR) spectrometer.

In the experiments, FELIX was tuned to the Si-O-Si asymmetric stretching mode wavelength at close to 10.42 μm ($\sim 960 \text{ cm}^{-1}$), which, due to the anharmonicity of the

vibrational potential and the spectral width of the FEL pulses (~ 43 nm or 40 cm^{-1}), induces motion on the fundamental resonance ($\nu=0 \rightarrow \nu=1$) only. Since FELIX is an rf linac FEL, it generates pulsed light with a macropulse-micropulse structure. The micropulses are variable in length from 500 fs to ~ 5 ps and have a repetition rate of 25 MHz in the experiments performed here. A 4-ms-long burst of micropulses comprises the macropulse, which have a repetition rate of either 10 or 5 Hz.

In the transient grating measurements, two noncollinear pump beams (with wave vectors \mathbf{k}_1 and \mathbf{k}_2) were spatially and temporally overlapped in the sample, creating a vibrational population grating. A weaker, spatially overlapped but time-delayed probe beam (with wave vector \mathbf{k}_3) is then Bragg-diffracted off this grating into a phase-matched signal direction ($\mathbf{k}_4 = \mathbf{k}_1 - \mathbf{k}_2 + \mathbf{k}_3$) with a signal intensity that decays as $T_1/2$ for variable delays, τ , between the fixed pump pulses and the probe. From the angle, θ_p , of 11.5° between the pump beams we deduce a grating period [$\lambda_p/2 \sin(\theta_p/2)$ with λ_p the pump wavelength] of 52 μm . The maximum grating efficiency $\eta(\tau)$ that could be observed at a zero delay between the pump and probe pulses was 1.82×10^{-3} at a total pump irradiance of 35.65 GW/cm^2 . Since the scattering efficiency for an optically thin refractive index grating is $\eta(\tau) \cong [k\Delta n(\tau)d/2]^2$ where k is the probe wavevector and d is the sample thickness, we can therefore infer a refractive index change of $\Delta n(0) = 0.133$. Relating this change to an effective nonlinear refractive coefficient n_2 [through $\Delta n(0) = n_2 I_0$, where I_0 is the pump beam irradiance] we obtain an n_2 value of 3.73×10^{-3} cm^2/GW .

The photon-echo measurement relies upon a two-pulse sequence that is applied to the sample such that the first pulse (with wave vector \mathbf{k}_1) creates a coherent superposition of vibrational states. Immediately after the first pulse all of the microscopic dipoles of the vibrational ensemble oscillate in phase. Due to the distribution of frequencies within the inhomogeneous line shape, the initial phase relation is rapidly lost via the free induction decay. A time τ later a second

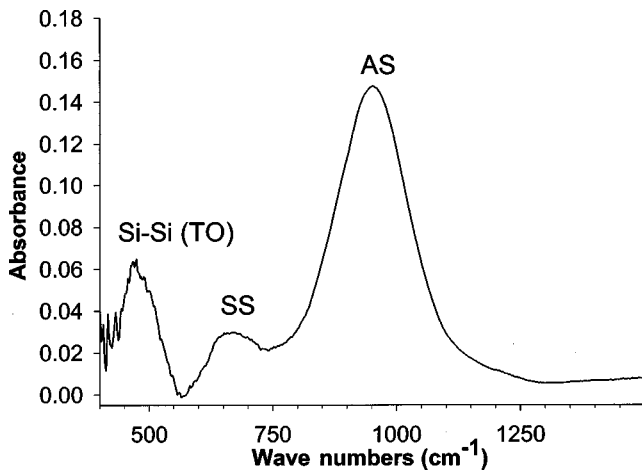


FIG. 1. Room-temperature infrared absorption spectrum of $a\text{-SiO}_{0.1}$. AS denotes the asymmetric stretching mode at 960 cm^{-1} . SS denotes the symmetric stretching mode at 670 cm^{-1} with the Si-Si (TO) peak also shown.

pulse (with wave vector \mathbf{k}_2) causes an inversion of the macroscopic dipole moment which leads to a rephasing of these individual frequency components, yielding, at an additional time τ , a phase-matched superradiant burst from the then rephased ensemble known as a photon echo. The time-integrated echo signal propagating along the $\mathbf{k}_{\text{echo}} = |\mathbf{k}_2 - \mathbf{k}_1|$ signal direction decays as a function of the delay between the incoming pulses with $T_2/4$.

III. RESULTS

Figure 1 shows the room-temperature Fourier-transform infrared absorption spectrum of $a\text{-SiO}_{0.1}$ in the $400\text{--}1500\text{-cm}^{-1}$ region obtained using a crystalline silicon background. The intense feature (labeled AS) centered around 960 cm^{-1} is the asymmetric stretch mode of the Si-O-Si complex and can be identified by analogy with the stoichiometric compound $a\text{-SiO}_2$ whose asymmetric stretch mode lies at 1076 cm^{-1} .⁹ A weaker feature at approximately 670 cm^{-1} is attributable to the symmetric stretch mode (labeled SS), while the absorption peak near 480 cm^{-1} is most probably the Si-Si TO mode peak.

Figure 2(a) shows the transient grating signal induced for resonant excitation of the AS mode at 10 K using $2\text{-}\mu\text{J}$ pump pulses. The decay profile fits well to a single exponential function [$\propto \exp(-2\tau/T_1)$], where τ is the delay between the

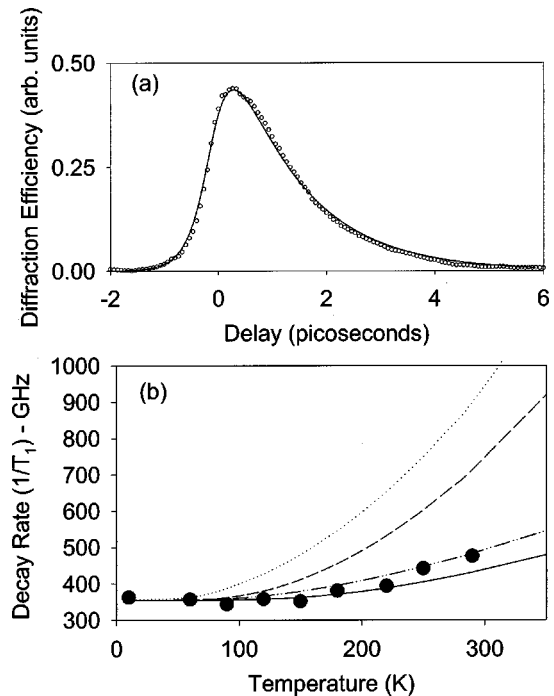


FIG. 2. (a) 10-K transient grating signal exciting the AS mode resonantly at 960 cm^{-1} . (b) Temperature-dependent population decay rate. The dotted line is a fit to Eq. (1) in the text with $[T_1(0)]^{-1} = 355$ GHz and for decay into 1 LA (320-cm^{-1}), 1 TA (160-cm^{-1}), and 1 TO (480-cm^{-1}) phonons. The dashed line is decay into three equal-energy 320-cm^{-1} LA phonons. The solid line is decay into two equal-energy 480-cm^{-1} TO phonons, while the dashed-dotted line is decay into a single Si-O-Si symmetric mode at 670 cm^{-1} + 1 LA mode at 290 cm^{-1} .

exciting pump pulses and the probe pulse], yielding a fast decay time of 2.8 ps. A sech function has been used to approximate the exciting FELIX pulse with a full width at half maximum of 710 fs. Figure 2(b) shows the temperature dependence of the decay rate (in GHz) which only increases by approximately 25% in the temperature range 10–300 K. We estimate that during the first 30 pulses (over which the signal was averaged), local heating at these incident power levels induces a temperature increase of up to 95 K. Of course, this estimate neglects the fact that not all of the energy absorbed stays in the laser focus over more than 1 μ s and it is unreasonable to suggest that all the energy absorbed is converted into heat. Clearly, the real temperature rise would be significantly less.

Theoretical models that describe the anharmonic break up of a particular vibrational mode, measured via the decay rate $[(T_1)^{-1}]$, do so in terms of the relationship between temperature T and the frequencies of the accepting modes ω_i , maintaining the appropriate energy conservation rule $\sum_i \hbar \omega_i = \hbar \omega$, where ω is the frequency of the initially excited mode. The temperature-dependent form for the energy decay rate is given by¹⁰

$$[T_1(T)]^{-1} = [T_1(0)]^{-1} \frac{\exp(\hbar \omega / k_B T) - 1}{\prod_i [\exp(\hbar \omega_i / k_B T) - 1]}, \quad (1)$$

where $[T_1(0)]^{-1}$ is the spontaneous decay rate (which we approximate by values at the lowest measured temperatures), $\hbar \omega$ is the Si-O-Si vibrational energy, k_B is Boltzmann's constant, and $\hbar \omega_i$ is the energy of the accepting modes into which the Si-O-Si vibration decays via process of order i . The spontaneous decay rate $[T_1(0)]^{-1}$ is taken to be 355 GHz, as determined from experiment. In Fig. 2(b) four different possibilities are shown for the various accepting modes. The dotted line shows three-phonon decay into 1 LA (320 cm^{-1}), 1 TA (160 cm^{-1}), and 1 TO (480 cm^{-1}) phonons. As can be seen, this does not account well for the data, activating too early due to the low frequency 160 cm^{-1} involved. Furthermore, three-phonon decay processes are likely to be unable to account for the residual decay rate of ~ 355 GHz due to the inherent inefficiency of such a high-order process. In fact, no possible combination of three phonons can remotely reproduce the data. Decay into three equal-energy LA phonons is shown as a dashed line in Fig. 2(b). However, decay into two accepting modes is an eminently reasonable proposition and 10-K vibrational lifetimes of the order of a few (2–5) picoseconds have been observed previously in decay processes attributable to two accepting phonon modes.^{11,12} The solid line in Fig. 2(b) represents decay into two equal-energy 480- cm^{-1} phonons, being the peak in the Si-Si one-phonon density of states, while the dashed-dotted line is decay into a single Si-O-Si symmetric mode at 670 cm^{-1} with 1 LA mode at 290 cm^{-1} bridging the energy mismatch. Due to the scatter in the data points, it is not possible to distinguish between the two decay pathways, although both give broad agreement with the observed temperature increase in the decay rate.

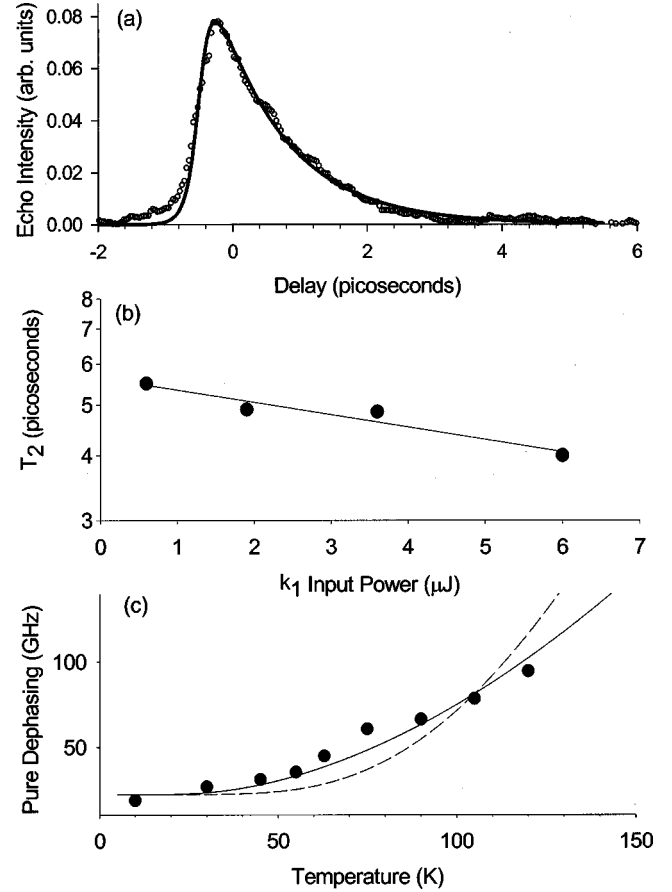


FIG. 3. (a) 10-K photon echo signal. (b) Power dependence of the homogeneous dephasing time. (c) Temperature dependence of the pure dephasing rate. The dashed line is a fit to Eq. (3) with $\theta_D = 450$ K, $a = 22$ GHz, and $A = 15$ THz. The solid line is a fit to Eq. (4) with $a = 22$ GHz and $A = 0.13$ THz.

The asymmetric stretch mode has a linewidth of ~ 75 cm^{-1} at room temperature, and hence the absorption line shape in amorphous silicon is undoubtedly massively inhomogeneously broadened, which precludes any possibility of obtaining information on relaxation processes in the frequency domain. The dynamic (or homogeneous) linewidth is characterized by the transverse decay constant T_2 . Contributions arise from both the anharmonic population decay and pure dephasing processes as embodied in the expression

$$\frac{1}{\pi T_2} = \frac{1}{\pi T_2^*} + \frac{1}{2\pi T_1}, \quad (2)$$

where T_2^* is the pure dephasing time arising from random forces exerted upon the Si-O-Si defect by the medium, producing fluctuations in the time-dependent vibrational eigenvalues. These fast fluctuations cause individual oscillators to lose phase with one another. It is the evolution of the system on scales substantially slower than T_2 , the homogeneous dephasing time, which gives rise to the inhomogeneous broadening. Consequently, to obtain information on the homogeneous line shape we must resort to nonlinear techniques

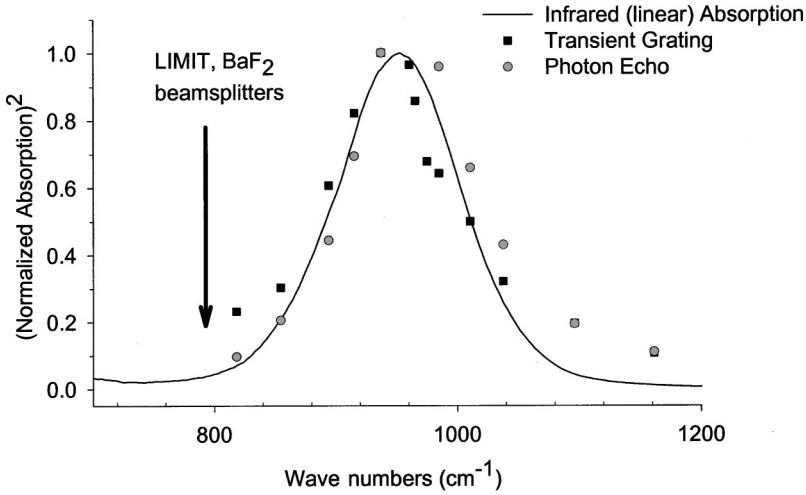


FIG. 4. The spectral dependence of the four-wave mixing amplitude compared against the squared absorption profile.

such as the vibrational echo, which are designed to remove the effects of inhomogeneous broadening.

In Fig. 3(a) we show the observed photon-echo signal measured at 10 K using similar incident power levels as were used in the transient grating measurement. The decay of the transient is shown to fit well to a single exponential function [$\propto \exp(-4\pi/T_2)$], yielding a homogeneous dephasing time of 4.5 ps. This corresponds to a homogeneous linewidth of $\sim 2.4 \text{ cm}^{-1}$ at 10 K, confirming that the signal observed here is an echo (as opposed to a four-wave mixing signal in a purely homogeneous system, which would decay as $T_2/2$ and should yield a linewidth equal to that observed in a linear absorption measurement¹³). A finite quantity of pure dephasing is present at 10 K and results from the presence of non-equilibrium phonons created in the anharmonic breakup of the AS mode itself, as has been observed in both hydrogenated and deuterated *a*-Si. In Fig. 3(b) we show one of the characteristic features of this behavior, which is the presence of a temperature-independent and incident-power-density-dependent component to the dephasing time measured. We note that excitation-induced dephasing (or instantaneous diffusion) could yield a finite contribution to pure dephasing at 10 K, however, in these diluted samples the distance between local oscillators is likely to be too great for this to be significant. Figure 3(c) shows the temperature dependence of the pure dephasing up to 120 K, beyond which insufficient temporal resolution was available. It is likely that the observed increase in the pure dephasing rate can be attributed to two-phonon elastic scattering by Si-Si phonons off the Si-O-Si complex. Under the assumption of a Debye-like distribution of Si-Si modes this process has a temperature-dependent form:

$$[T_2^*(T)]^{-1} = a + A \left(\frac{T}{\theta_D} \right)^7 \int_0^{\theta_D/T} \frac{x^3}{(e^x - 1)} dx, \quad (3)$$

where a is a constant which describes the residual dephasing induced by nonequilibrium phonons, A is a phonon coupling constant, and θ_D is the Debye temperature that has been set equal to 450 K. The dashed line in Fig. 3(c) is a fit to this

expression with $a = 22 \text{ GHz}$ and $A = 15 \text{ THz}$. As can be seen, this completely underestimates the activation temperature of the dephasing. However, a model of dephasing via a single mode can account for the data. In this case we have

$$[T_2^*(T)]^{-1} = a + A n_\omega (n_\omega + 1), \quad (4)$$

where n_ω is the Bose-Einstein occupancy factor. The solid curve in Fig. 3(c) is a fit to this expression for a 100-cm^{-1} mode with $a = 22 \text{ GHz}$ as before and $A = 0.13 \text{ THz}$. The large reduction in the dephasing constant is necessary due to the low-energy 100-cm^{-1} TA mode contributing to the temperature-dependent dephasing. We note that this value is comparable to that observed for the Si-D stretch mode in deuterated amorphous silicon of 0.27 THz .⁷

In order to confirm that these nonlinear signals were indeed associated with the nonlinear susceptibility of the AS mode in *a*-SiO_{0.1} we have measured the spectral dependence of the nonlinear signal amplitude and compared this with the square of the absorption strength to which they should be proportional. As is shown in Fig. 4, the spectral dependence of the transient grating and photon echo amplitude matches the squared absorption line profile well. Furthermore no signals could be generated in a sample consisting of a *c*-Si substrate (taken from wafers grown under analogous conditions) alone.

IV. CONCLUSIONS

Measurements of the population decay of the asymmetric stretch mode in *a*-Si:O_{0.1} reveal fast dynamics with a 10-K lifetime of 2.8 ps determined from transient grating spectroscopy. From the temperature dependence of the decay rate it is possible to infer that stimulated emission of two accepting modes is responsible for the observed behavior. Two-pulse photon echo spectroscopy yields a 10-K homogeneous linewidth of 2.4 cm^{-1} . The temperature dependence of the dephasing rate is governed by elastic phonon scattering events with a small contribution from nonequilibrium phonons, as has been observed previously for hydrogen and deuterium vibrations in this material.

ACKNOWLEDGMENTS

The authors gratefully acknowledge the support of the Stichting voor Fundamenteel Onderzoek der Materie (FOM) in providing the required beamtime on FELIX as a part of the FOM-EPSC collaborative condensed matter physics

program and highly appreciate the skillful assistance of the FELIX staff, in particular Dr. Lex van der Meer. J.P.R.W. would like to thank the FELIX free-electron laser facility for financially supporting his visit to the Netherlands in order to pursue this research.

*Corresponding author. Email address: j.p.wells@sheffield.ac.uk

¹A. Polman and R. G. Elliman, in *Towards the First Silicon Laser*, NATO Science Series Volume, edited by L. Pavesi, S. Gaponenko, and L. Dal Negro (Kluwer, Amsterdam, 2003).

²L. Khriachtchev, S. Novikov, and J. Lahtinen, *J. Appl. Phys.* **92**, 5856 (2002).

³C. L. Pavesi, L. Dai Negro, C. Mazzoleni, G. Franzò, and F. Priolo, *Nature (London)* **408**, 440 (2000).

⁴J. Ni and E. Arnold, *Appl. Phys. Lett.* **39**, 554 (1981).

⁵J. J. van Hapert, E. E. van Faassen, W. M. Arnoldbik, N. Tomozeiu, A. M. Vredenberg, and F. H. P. M. Habraken (unpublished).

⁶M. van der Voort, C. W. Rella, L. F. G. van der Meer, A. V. Akimov, and J. I. Dijkhuis, *Phys. Rev. Lett.* **84**, 1236 (2000).

⁷J.-P. R. Wells, R. E. I. Schropp, L. F. G. van der Meer, and J. I. Dijkhuis, *Phys. Rev. Lett.* **89**, 125504 (2002).

⁸G. Lucovsky and W. B. Pollard, in *Topics in Applied Physics*, edited by J. D. Joannopoulos and G. Lucovsky (Springer, Berlin, 1984), Vol. 56, pp. 301–355.

⁹C. T. Kirk, *Phys. Rev. B* **38**, 1255 (1988).

¹⁰A. Nitzan, S. Mukamel, and J. Jortner, *J. Chem. Phys.* **60**, 3929 (1974).

¹¹J.-P. R. Wells, I. V. Bradley, G. D. Jones, and C. R. Pidgeon, *Phys. Rev. B* **64**, 144303 (2001).

¹²G. D. Jones and J.-P. R. Wells, *J. Lumin.* **102-103**, 169 (2003).

¹³J.-P. R. Wells, C. W. Rella, I. V. Bradley, I. Galbraith, and C. R. Pidgeon, *Phys. Rev. Lett.* **84**, 4998 (2000).